NASA

National Aeronautics and
Space Administration

NASA CR-165439

# EDGE DELAMINATION IN ANGLE-PLY COMPOSITE LAMINATES

DTIC
SELECTE
DEC 2 8 1995
F

Final Report - Part V

DISTRIBUTION STATEMENT A
Approved for public release;
Distribution Unlimited

by

S.S. Wang

Department of Theoretical and Applied Mechanics
UNIVERSITY OF ILLINOIS
at Urbana-Champaign

DEPARTMENT OF DEFENSE
PLASTICS TECHNICAL EVALUATION CENTER
ARRADCOM, DOVER, N. J. 07801

prepared for

NATIONAL AERONAUTICS AND SPACE ADMINISTRATION

19951226 073

NASA Lewis Research Center
Grant NSG 3044

DTIC QUALITY INSPECTED 1

PLASTEC 48/88

| 1. Report No. | 2. Government Accession No. | 3. Recipient's Catalog No. |
|---|---|---|
| NASA CR 165439 | | |

| 4. Title and Subtitle | 5. Report Date |
|---|---|
| Edge Delamination In Angle-ply Composite Laminates | February 1981 |
| | 6. Performing Organization Code |

| 7. Author(s) | 8. Performing Organization Report No. |
|---|---|
| S. S. Wang | |
| | 10. Work Unit No. |

| 9. Performing Organization Name and Address | 11. Contract or Grant No. |
|---|---|
| University of Illinois<br>Urbana, IL 61801 | NSG 3044 |
| | 13. Type of Report and Period Covered |
| 12. Sponsoring Agency Name and Address<br>National Aeronautics and Space Administration<br>Washington DC 20546 | Final Report - Part V |
| | 14. Sponsoring Agency Code |

15. Supplementary Notes

Project Manager: C. C. Chamis, Structures & Mechanical Technologies Division
NASA Lewis Research Center, Mail Stop 49-6
21000 Brookpark Road
Cleveland, OH 44135

16. Abstract

A theoretical method has been developed for describing the edge delamination stress intensity characteristics in angle-ply composite laminates. The method is based on the theory of anisotropic elasticity. The edge delamination problem is formulated using Lekhnitskii's complex-variable stress potentials and an especially developed eigenfunction expansion method. The method predicts exact orders of the three-dimensional stress singularity in a delamination crack tip region. With the aid of boundary collocation, the method predicts the complete stress and displacement fields in a finite-dimensional, delaminated composite. Fracture mechanics parameters such as the mixed-mode stress intensity factors and associated energy release rates for edge delamination can be calculated explicity. Solutions are obtained for edge delaminated $(\theta/-\theta\ -\theta/\theta)$ angle-ply composites under uniform axial extension. Effects of delamination lengths, fiber orientations, lamination and geometric variables are studied in detail.

| 17. Key Words (Suggested by Author(s)) | 18. Distribution Statement |
|---|---|
| stress intensity, energy release-rate, anisotropy, elasticity, complex variables, eigen expansion, collocation, mix-modes, 3-D stress-analysis | Unclassified, Unlimited |

| 19. Security Classif. (of this report) | 20. Security Classif. (of this page) | 21. No. of Pages | 22. Price* |
|---|---|---|---|
| Unclassified | Unclassified, Unlimited | | |

* For sale by the National Technical Information Service, Springfield, Virginia 22161

TABLE OF CONTENTS

## FOREWORD

This report describes a portion of the results obtained on NASA Grant NSG 3044. This work was done under subcontract to the University of Illinois, Urbana, with Prof. S.S. Wang as the Principal Investigator. The prime grantee was the Massachusetts Institute of Technology, with Prof. F.J. McGarry as the Principal Investigator and Dr. J.F. Mandell as a major participant. The NASA - LeRC Project Manager was Dr. C.C. Chamis.

Efforts in this project are primarily directed towards the development for finite element analyses for the study of flaw growth and fracture of fiber composites. This report presents exact solutions for edge delaminations in angle-ply composites.


| Accesion For | |
|---|---|
| NTIS CRA&I | ☒ |
| DTIC TAB | ☐ |
| Unannounced | ☐ |
| Justification | |
| By | |
| Distribution / | |
| Availability Codes | |
| Dist | Avail and / or Special |
| A-1 | |

## ABSTRACT

Edge delamination has caused severe concern in the design and analysis of advanced composite materials and structures. Due to its complex nature, very limited knowledge for the problem is currently available. It involves not only geometric and material discontinuities but also inherently coupled mode I, II and III fracture in the layered anisotropic system. Based on complex-variable stress potentials in the anisotropic elasticity theory and eigenfunction expansion, exact orders of the crack-tip stress singularity and complete field solutions are obtained. Results are given for edge-delaminated composites subjected to uniform axial extension for illustrative purposes. Effects of geometric, lamination, and crack variables are determined.

# 1. INTRODUCTION

Edge delamination is frequently encountered in angle-ply composite laminates. It is due to high stress concentrations at geometric boundaries and the inherently weak interlaminar strength along the ply interface. The problem posed by edge delamination is of great theoretical interest. It also is of significant technical importance in determining the structural integrity and damage tolerance of advanced fiber-reinforced composites and their applications to advanced engineering structures and components. The presence and growth of delamination cracks from geometric boundaries of composite laminates may lead to severe reliability and safety problems of fiber composite materials and structures such as the reduction of structural stiffness, the exposure of the interior to adverse environmental attack, and the disintegration of the material, which may cause the final failure. Thus, understanding the basic nature of edge delamination is of critical importance in damage characterization and accurate assessment of flaw criticality and structural integrity of advanced composites.

The edge delamination problem is very complex in nature and extremely difficult to solve. It involves geometric and materials discontinuities, i.e., free edges, interlaminar cracks and variation of ply properties in the transverse direction. It also involves inherently coupled mode I, II and III fracture in the anisotropic layered material system such as angle-ply composite laminates. Edge delamination is basically a fracture problem involving an interfacial

crack between two highly anisotropic fiber-composite laminae under general loading conditions. The problem of an interfacial crack between two dissimilar isotropic materials has received much attention recently, for example, Refs. [1-12]. But the study of a delamination between strongly anisotropic fiber composite layers, especially in finite-dimensional laminates under general loading, has been very limited, to the author's knowledge. In this paper, a rigorous investigation of the basic nature of the coupled opening, sliding and antiplane shearing fracture behavior of edge delamination is presented for composite laminates under uniform axial extension. Basic formulation of the problem based on the theory of anisotropic elasticity and eigenfunction expansion is given in the next section. General solutions and associated stress singularities for the edge delamination are derived in Section 3. Fracture parameters such as mixed-mode stress intensity factors $K_I$, $K_{II}$ and $K_{III}$ as well as the energy release rate G are defined and determined in Section 4. Numerical results for edge delaminated composite laminates subjected to uniform axial loading are shown in Section 5 to illustrate the fundamental behavior of edge delamination cracks. Effects of geometric, lamination and crack variables are studied in detail.

## 2. FORMULATION

Formulation of the delamination problem is based on the theory of anisotropic elasticity for nonhomogeneous solids. Well known Lekhnitskii's stress functions [13] are introduced to establish governing partial differential equations for field variables. An eigenfunction expansion method is employed for determining the stress singularity at the delamination crack tip. The boundary collocation technique is then used to evaluate the complete solution for finite-dimensional composite laminates.

### 2.1 Assumptions and Delamination Model

Consider a composite laminate (Fig. 1) composed of unidirectional fiber-reinforced plies of uniform thicknesses, $h_1$, $h_2$,....$h_n$. For simplicity but without loss of generality, we restrict ourself to the cases of symmetric, angle-ply composite laminates with fiber orientations $(\theta_1/\theta_2/..../\theta_2/\theta_1)$. Ply thicknesses are also assumed to be symmetric with respect to the x-z plane, i.e., $h_1 = h_n$, $h_2 = h_{n-1}$, .... The composite has a finite width 2b and is subjected to a uniform axial extension, $e$, where $e$ = constant, along the z-axis. The composite laminate is sufficiently long that, in the region far away from the ends, end effects are negligible by virtue of the Saint Venant principle. Consequently, stresses in the laminate are independent of the z-axis. The case in which stresses and displacements are independent of z corresponds to the well known generalized plane deformation [13]. Edge delamination occurs in the form of a crack along the interface of dissimilar plies with fiber orientations, $\theta_k$ and $\theta_{k+1}$.

Perfect bonding is assumed in the composite everywhere except the region of delamination.

## 2.2 Basic Equations

For each individual lamina, the constitutive equations in the structural coordinates x-y-z may be expressed by the generalized Hooke's law in the contracted notation as

$$\varepsilon_i = S_{ij}\,\sigma_j \qquad (i,j = 1,2,....6) \tag{1}$$

where $\varepsilon_i$ and $\sigma_j$ are strain and stress tensors, and $S_{ij}$, the compliance tensors, respectively. The strain-displacement relationships are given by

$$\varepsilon_1 = \varepsilon_x = u_{,x}, \qquad \varepsilon_2 = \varepsilon_y = v_{,y}, \tag{2a-b}$$

$$\varepsilon_3 = \varepsilon_z = w_{,z}, \qquad \varepsilon_4 = \gamma_{yz} = w_{,y} + v_{,z}, \tag{2c-d}$$

$$\varepsilon_5 = \gamma_{xz} = w_{,x} + u_{,z}, \quad \varepsilon_6 = \gamma_{xy} = u_{,y} + v_{,x}, \tag{2e-f}$$

where the subscript after comma denotes the partial differentiation with respect to the variable. Under these assumptions, there remain three compatability relations:

$$\varepsilon_{x,yy} + \varepsilon_{y,xx} = \gamma_{xy,xy}, \tag{3a}$$

$$(-\gamma_{xz,y} + \gamma_{yz,x})_{,y} = 0, \tag{3b}$$

$$(-\gamma_{yz,x} + \gamma_{xz,y})_{,x} = 0. \tag{3c}$$

For a symmetrical angle-ply composite laminate subjected to uniform axial strain $e$, it can be shown easily that

$$\gamma_{xz,_y} - \gamma_{yz,_x} = 0, \tag{4}$$

since the relative angle of rotation for the symmetric composite laminate about z-axis vanishes.

Based on the definition of the problem, i.e., $\varepsilon_z = e$ = constant, $\sigma_z$ in Eq 1 can be expressed in terms of other stress components by

$$\sigma_z = (e - S_{3j}\,\sigma_j)/S_{33} \qquad (j = 1,2,4,5,6). \tag{5}$$

Thus, the generalized Hooke's law may be modified to have the following form:

$$\varepsilon_i = \tilde{S}_{ij}\,\sigma_j + e_i \qquad (i,j = 1,2,4,5,6), \tag{6a}$$

where

$$\tilde{S}_{ij} = S_{ij} - S_{3i}S_{3j}/S_{33}, \qquad e_i = eS_{i3}/S_{33} \qquad (i,j \neq 3). \tag{6b}$$

It can be seen from Eq 6 that $e_i$ has the role of initial strains in the laminate. For the current stress formulation, it may be more convenient to introduce the initial stress $\sigma_{jo}$ such that

$$\varepsilon_i = \tilde{S}_{ij}(\sigma_j - \sigma_{jo}), \qquad (i,j = 1,2,4,5,6), \tag{7}$$

where $\sigma_{io} = -\tilde{S}^{-1}_{ij}\,e_j$. It is possible to decompose the complete solutions into two parts, i.e.,

$$\sigma_i = \sigma_i^{(h)} + \sigma_j^{(p)} \tag{8a}$$

$$\varepsilon_i = \varepsilon_i^{(h)} + \varepsilon_j^{(p)} \tag{8b}$$

where

$$\varepsilon_i^{(h)} = \tilde{S}_{ij}\,\sigma_j^{(h)} \quad \text{and} \quad \varepsilon_i^{(p)} = \tilde{S}_{ij}(\sigma_j^{(p)} - \sigma_{jo}). \tag{9a-b}$$

## 3. GENERAL SOLUTIONS AND ASSOCIATED STRESS SINGULARITIES FOR DELAMINATION

### 3.1 Solutions for $\sigma_i^{(h)}$ and $u_i^{(h)}$

Introducing the stress functions $F(x,y)$ and $\Psi(x,y)$ which satisfy equations of equilibrium identically and following the procedure by Lekhnitskii [13], we obtain a pair of coupled partial differential equations as follows:

$$\begin{cases} L_4 F + L_3 \Psi = 0, & \text{(10a)} \\ L_3 F + L_2 \Psi = 0, & \text{(10b)} \end{cases}$$

where $L_2$, $L_3$ and $L_4$ are linear differential operators of the second, third and fourth order, respectively, defined by

$$L_2 = \tilde{S}_{44} \frac{\partial^2}{\partial x^2} - 2\tilde{S}_{45} \frac{\partial^2}{\partial x \partial y} + \tilde{S}_{55} \frac{\partial^2}{\partial y^2}, \qquad \text{(10c)}$$

$$L_3 = -\tilde{S}_{24} \frac{\partial^3}{\partial x^3} + (\tilde{S}_{25} + \tilde{S}_{46}) \frac{\partial^3}{\partial x^2 \partial y} - (\tilde{S}_{14} + \tilde{S}_{56}) \frac{\partial^3}{\partial x \partial y^2} + \tilde{S}_{15} \frac{\partial^3}{\partial y^3}, \qquad \text{(10d)}$$

$$L_4 = \tilde{S}_{22} \frac{\partial^4}{\partial x^4} - 2\tilde{S}_{26} \frac{\partial^4}{\partial x^3 \partial y} + (2\tilde{S}_{12} + \tilde{S}_{66}) \frac{\partial^4}{\partial x^2 \partial y^2} - 2\tilde{S}_{16} \frac{\partial^4}{\partial x \partial y^3} + \tilde{S}_{11} \frac{\partial^4}{\partial y^4}. \qquad \text{(10e)}$$

Lekhnitskii [13] has shown that the general solution for Eqs 10a-10b may be expressed as

$$F(Z_k) = \sum_{k=1}^{6} F_k(Z_k), \qquad \Psi(Z_k) = \sum_{k=1}^{6} \eta_k F_k'(Z_k), \qquad \text{(11a-b)}$$

where $Z_k = x + \mu_k y$; the prime (') denotes differentiation of the function $F_k$ with respect to its argument; and $\mu_k$ are the roots of the algebraic characteristic equation

$$\ell_4(\mu)\ell_2(\mu) - \ell_3^2(\mu) = 0, \tag{12a}$$

and

$$\eta_k = -\ell_3(\mu_k)/\ell_2(\mu_k) = -\ell_4(\mu_k)/\ell_3(\mu_k), \tag{12b}$$

with

$$\ell_2(\mu) = \tilde{S}_{55}\mu^2 - 2\tilde{S}_{45}\mu + \tilde{S}_{44}, \tag{13a}$$

$$\ell_3(\mu) = \tilde{S}_{15}\mu^3 - (\tilde{S}_{14} + \tilde{S}_{56})\mu^2 + (\tilde{S}_{25} + \tilde{S}_{46})\mu - \tilde{S}_{24}, \tag{13b}$$

$$\ell_4(\mu) = \tilde{S}_{11}\mu^4 - 2\tilde{S}_{16}\mu^3 + (2\tilde{S}_{12} + \tilde{S}_{66})\mu^2 - 2\tilde{S}_{26}\mu + \tilde{S}_{22}. \tag{13c}$$

Introducing the following form for the function $F_k(Z_k)$

$$F_k(Z_k) = C_k Z_k^{\delta+2}/[(\delta + 2)(\delta + 1)], \tag{14}$$

where $C_k$ and $\delta$ are arbitrary complex constants to be determined later, we can obtain the stress and displacement expressions as follows:

$$\sigma_x^{(h)} = \sum_{k=1}^{3} [C_k \mu_k^2 Z_k^\delta + C_{k+3}\, \overline{\mu}_k^2\, \overline{Z}_k^\delta], \tag{15a}$$

$$\sigma_y^{(h)} = \sum_{k=1}^{3} [C_k Z_k^\delta + C_{k+3}\, \overline{Z}_\kappa^\delta], \tag{15b}$$

$$\tau_{yz}^{(h)} = -\sum_{k=1}^{3} [C_k \eta_k Z_k^\delta + C_{k+3}\, \overline{\eta}_k\, \overline{Z}_k^\delta], \tag{15c}$$

$$\tau_{xz}^{(h)} = \sum_{k=1}^{3} [C_k \mu_k \eta_k Z_k^\delta + C_{k+3}\, \overline{\mu}_k\, \overline{\eta}_k\, \overline{Z}_k^\delta], \tag{15d}$$

$$\tau_{xy}^{(h)} = -\sum_{k=1}^{3} [C_k \mu_k Z_k^{\delta} + C_{k+3} \bar{\mu}_k \bar{Z}_k^{\delta}], \tag{15e}$$

and

$$u^{(h)} = \sum_{k=1}^{3} [C_k p_k Z_k^{\delta+1} + C_{k+3} \bar{p}_k \bar{Z}_k^{\delta+1}]/(\delta + 1) \tag{16a}$$

$$v^{(h)} = \sum_{k=1}^{3} [C_k q_k Z_k^{\delta+1} + C_{k+3} \bar{q}_k \bar{Z}_k^{\delta+1}]/(\delta + 1) \tag{16b}$$

$$w^{(h)} = \sum_{k=1}^{3} [C_k t_k Z_k^{\delta+1} + C_{k+3} \bar{t}_k \bar{Z}_k^{\delta+1}]/(\delta + 1) \tag{16c}$$

where

$$p_k = \tilde{S}_{11}\mu_k^2 + \tilde{S}_{12} - \tilde{S}_{14}\eta_k + \tilde{S}_{15}\eta_k\mu_k - \tilde{S}_{16}\mu_k \tag{16d}$$

$$q_k = \tilde{S}_{12}\mu_k + \tilde{S}_{22}/\mu_k - \tilde{S}_{24}\eta_k/\mu_k + \tilde{S}_{25}\eta_k - \tilde{S}_{26}\ , \tag{16e}$$

$$t_k = \tilde{S}_{14}\mu_k + \tilde{S}_{24}/\mu_k - \tilde{S}_{44}\eta_k/\mu_k + \tilde{S}_{45}\eta_k - \tilde{S}_{46}\ . \tag{16f}$$

The constant, $\delta$, in Eqs 15 and 16 may be chosen that the stresses and displacements $\sigma_i^{(h)}$ and $u_i^{(h)}$ satisfy interface continuity and homogeneous boundary conditions. Taking complex conjugate of Eqs 15 and 16, their forms are invariant; thus, $\delta$ appears as a set of complex conjugates, which enables to make Eqs 15 and 16 real functions by superposition. Furthermore, finiteness of displacements at the origin requires that $\mathrm{Re}[\delta] > -1$, where Re represents the real part of $\delta$.

## 3.2 Solutions for $\sigma_i^{(p)}$ and $u_i^{(p)}$

Since $\sigma_{io}$ and $e_i$ in Eqs 6 and 7 are constant, we may choose $\sigma_i^{(p)}$ in Eq 9 as constants so that they satisfy the equations of equilibrium

and compatibility conditions identically. For each individual lamina, let $\sigma_i^{(p)}$ take the following form:

$$\sigma_x^{(p)} = \sigma_{xo} + \sum_{k=1}^{3} (d_k \mu_k^2 + \bar{d}_k \bar{\mu}_k^2), \tag{17a}$$

$$\sigma_y^{(p)} = \sigma_{yo} + \sum_{k=1}^{3} (d_k + \bar{d}_k), \tag{17b}$$

$$\tau_{yz}^{(p)} = \tau_{yzo} - \sum_{k=1}^{3} (d_k \eta_k + \bar{d}_k \bar{\eta}_k), \tag{17c}$$

$$\tau_{xz}^{(p)} = \tau_{xzo} + \sum_{k=1}^{3} (d_k \eta_k \mu_k + \bar{d}_k \bar{\eta}_k \bar{\mu}_k), \tag{17d}$$

$$\tau_{xy}^{(p)} = \tau_{xyo} - \sum_{k=1}^{3} (d_k \mu_k + \bar{d}_k \bar{\mu}_k). \tag{17e}$$

Substiuting Eqs 17a-17e into Eq 9b and integrating the strain-displacement relations, we obtain

$$u^{(p)} = \sum_{k=1}^{3} (d_k p_k Z_k + \bar{d}_k \bar{p}_k \bar{Z}_k) - \omega_3 y + \omega_2 z + u_o \tag{18a}$$

$$v^{(p)} = \sum_{k=1}^{3} (d_k q_k Z_k + \bar{d}_k \bar{q}_k \bar{Z}_k) + \omega_3 x - \omega_1 z + v_o, \tag{18b}$$

$$w^{(p)} = \sum_{k=1}^{3} (d_k t_k Z_k + \bar{d}_k \bar{t}_k \bar{Z}_k) - \omega_2 x + \omega_1 y + e z + w_o, \tag{18c}$$

where $u_o$, $v_o$, $w_o$ and $\omega_i$ are related to rigid-body displacements and rotations. The complex constants $d_k$ are required to satisfy the near-field traction boundary conditions and continuity conditions along the ply interface.

## 3.3 Delamination Crack-Tip Stress Singularity

Consider a delamination between two plies, say the kth and (k+1)th ply, in a composite subjected to general loading as shown in Fig. 2. Assuming that interlaminar crack surfaces are free from traction, we introduce the following boundary conditions for the eigen stresses $\sigma_i^{(h)}$:

$$\sigma_y^{(i)} = \tau_{yz}^{(i)} = \tau_{xy}^{(i)} = 0 \qquad (i = k,\ \phi = \pi;\ i = k+1,\ \phi = -\pi). \tag{19}$$

The superscript h is dropped in the expression for convenience.

Continuity conditions for displacements and interlaminar stresses along the interface, $\phi = 0$,

$$\{\sigma_y^{(k)}, \tau_{yz}^{(k)}, \tau_{xy}^{(k)}\} = \{\sigma_y^{(k+1)}, \tau_{yz}^{(k+1)}, \tau_{xy}^{(k+1)}\} \tag{20a}$$

$$\{u^{(k)}, v^{(k)}, w^{(k)}\} = \{u^{(k+1)}, v^{(k+1)}, w^{(k+1)}\}. \tag{20b}$$

Substituting Eqs 15 and 16 into 19 and 20, we obtain the following twelve linear algebraic equations in $C_m^{(k)}$ and $C_m^{(k+1)}$:

$$\sum_{m=1}^{3} \{e^{i\pi\delta} C_m^{(k)} \Gamma_{jm}^{(k)} + e^{-i\pi\delta} C_{m+3}^{(k)} \bar{\Gamma}_{jm}^{(k)}\} = 0, \qquad (j=1,2,3) \tag{21a}$$

$$\sum_{m=1}^{3} \{e^{-i\pi\delta} C_m^{(k+1)} \Gamma_{jm}^{(k+1)} + e^{i\pi\delta} C_{m+3}^{(k+1)} \bar{\Gamma}_{jm}^{(k+1)}\} = 0 \quad (j=1,2,3), \tag{21b}$$

$$\sum_{m=1}^{3} \{C_m^{(k)} \Gamma_{rm}^{(k)} + C_{k+3}^{(k)} \bar{\Gamma}_{rm}^{(k)}\} = \sum_{m=1}^{3} \{C_m^{(k+1)} \Gamma_{rm}^{(k+1)} + C_{m+3}^{(k+1)} \bar{\Gamma}_{rm}^{(k+1)}\}$$

$$(r=1,2,3,4,5,6), \tag{21c}$$

where $\Gamma_{1m}^{(k)}=1$, $\Gamma_{2m}^{(k)} = \eta_m^{(k)}$, $\Gamma_{3m}^{(k)} = \mu_m^{(k)}$, $\Gamma_{4m}^{(k)} = p_m^{(k)}$, $\Gamma_{5m}^{(k)} = q_m^{(k)}$ and $\Gamma_{6m}^{(k)} = t_m^{(k)}$. Solving Eqs 21c for $C_m^{(k)}$ and substituting the resulting

expressions into Eqs 21a, we get

$$\sum_{n=1}^{6} \{C_n^{(k+1)} \sum_{m=1}^{3} [e^{i\pi\delta} a_{mn} \Gamma_{jm}^{(k)} + e^{-i\pi\delta} a_{(m+3)n} \bar{\Gamma}_{jm}^{(k)}]\} = 0. \tag{21d}$$

Equations 21b and 21d consist of a system of six linear homogeneous algebraic equations. For nontrival solutions of $C_m^{(k+1)}$, the determinant of coefficients of the algebraic equations must vanish. This leads to a characteristic equation of the following form:

$$(e^{i2\pi\delta} - 1)^3 |\Delta(\delta)| = 0, \tag{22}$$

where $|\Delta(\delta)|$ is a 3 by 3 determinant involving $\delta$ in a transcendental form and material constants, $\mu_m^{(k)}$, $\eta_m^{(k)}$ and $\mu_m^{(k+1)}$, $\eta_m^{(k+1)}$ of the adjacent layers. Details of $\Delta(\delta)$ may be found in Ref. [14]. The general form of $\delta$, which are the eigenvalues of the problem, may be written as

$$\delta_n = n, \quad \text{or} \quad \delta_n = (n - \tfrac{1}{2}) \pm i\gamma \qquad (n=0,1,2,\ldots), \tag{23}$$

where $\gamma$ is a constant related to elastic constants of adjacent plies. Thus, for each $\delta_n$ we have the eigenfunctions of the form Eqs 15 and 16 whose coefficients may be determined from the remote boundary conditions other than Eq 19. It is important to note that the $\delta_n$ bounded by

$$0 > \mathrm{Re}[\delta_n] > -1 \tag{24}$$

characterize the inherent stress singularities of the delamination crack stresses in a composite laminate.

For cross-ply composite laminates, the differential operator $L_3$ vanishes identically. Thus, $F(Z)$ and $\Psi(Z)$ are uncoupled, and the form

of Eq 23 can be simplified and expressed explicitly as

$$\delta_n = n, \quad \text{or}$$

$$\delta_n = (n - \tfrac{1}{2}) \pm \frac{i}{2\pi} \ln\{[b + (b^2 - 4a^2)^{\frac{1}{2}}]/(2a)\}, \tag{25}$$

where a and b are related to material constants $\tilde{S}_{ij}^{(k)}$, $\tilde{S}_{ij}^{(k+1)}$, $\mu_i^{(k)}$, $\bar{\mu}_i^{(k)}$ and $\mu_i^{(k+1)}$, $\bar{\mu}_i^{(k+1)}$ shown in Appendix 1. In a limiting case of isotropic materials, it can be shown that $\delta_n$ have the form,

$$\delta_n = (n - \tfrac{1}{2}) \pm \frac{i}{2\pi} \ln\{[G^{(k)} + G^{(k+1)}(3 - 4\nu^{(k)})]$$

$$/[G^{(k+1)} + G^{(k)}(3 - 4\nu^{(k+1)})]\}, \tag{26}$$

where G and $\nu$ denote the shear modulus and Poisson's ratio, respectively. The eigenvalues of Eq 26 were first obtained by William [1] and later by Zak, at al. [2] for interfacial cracks in isotropic media.

## 4. DELAMINATION STRESS INTENSITY FACTORS AND ENERGY RELEASE RATES

The eigenfunctions and the unknown constants for $\sigma_i^{(h)}$ and $\sigma_i^{(p)}$ in Eqs 15 and 17 are determined by imposing appropriate (materials and geometric) symmetry and traction boundary conditions, which will be discussed later. Hence, complete stresses and displacements $\sigma_i^{(\alpha)}$ and $u_i^{(\alpha)}$ in the $\alpha$-th lamina can be fully established. Neglecting the higher-order terms, we note that the typical structure of near-field crack tip stresses can be shown to have the following form:

$$\sigma_i^{(\alpha)} = \sum_{j=1}^{n} \sum_{k=1}^{3} [f_{ijk}^{(\alpha)} Z_k^{\delta_j} + g_{ijk}^{(\alpha)} \overline{Z}_k^{\delta_j}], \tag{27}$$

where $f_{ijk}^{(\alpha)}$ and $g_{ijk}^{(\alpha)}$ are related to the material constants, geometry, and boundary conditions; $\delta_j$ are eigenvalues bounded by $-1 < \mathrm{Re}[\delta_j] < 0$ to insure the positive definiteness of strain energy of the elastic body. It is clear that the eigenvalues which satisfy Eq 24 lead to asymptotic near field stresses. For the convenience of further development, the stress $\sigma_i^{(\alpha)}$ around the crack tip may be re-written as

$$\sigma_i^{(\alpha)} = \sum_{j=1}^{n} \sigma_{ij}^{(\alpha)}(x,y;\delta_j) + 0(\text{non-singular, higher-order terms}), \tag{28}$$

where $\sigma_{ij}^{(\alpha)}$ is the j-th singular component of the stress $\sigma_i^{(\alpha)}$ corresponding to the eigenvalue $\delta_j$ which meets Eq. 24.

In the context of mechanics of fracture, it is possible to define the so-called stress intensity factors for the delamination in a manner analogous to that given in Refs. [4,6] by considering the interlaminar stresses ahead of the crack tip along the interface, i.e.,

$$K_I = \lim_{x\to 0^+} \sum_{j=1}^{n} \sqrt{2\pi}\, x^{-\delta_j} \sigma_{2j}(x,0;\delta_j), \tag{29a}$$

$$K_{II} = \lim_{x\to 0^+} \sum_{j=1}^{n} \sqrt{2\pi}\, x^{-\delta_j} \sigma_{6j}(x,0;\delta_j), \tag{29b}$$

$$K_{III} = \lim_{x\to 0^+} \sum_{j=1}^{n} \sqrt{2\pi}\, x^{-\delta_j} \sigma_{4j}(x,0;\delta_j) \tag{29c}$$

where the superscript $\alpha$ is omitted, because tractions, $\sigma_2$, $\sigma_4$ and $\sigma_6$, are continuous across the interface.

While the stress intensity factors $K_I$, $K_{II}$ and $K_{III}$ describe the details of the delamination crack-tip field, the strain energy release rate G is also of significant interest, since this is a quantity physically measurable in experiments and mathematically well defined. The fracture energy release rate in a delaminated composite may be evaluated by using Irwin's virtual crack extension expression [15],

$$\begin{aligned} G &= G_I + G_{II} + G_{III} \\ &= \lim_{\delta\beta\to 0} \frac{1}{2\delta\beta} \int_0^{\delta\beta} \{\sigma_y(r,0)[v^{(k)}(\delta\beta-r,\pi) - v^{(k+1)}(\delta\beta-r,-\pi)] \\ &\quad + \tau_{xy}(r,0)[u^{(k)}(\delta\beta-r,\pi) - u^{(k+1)}(\delta\beta-r,-\pi)] \\ &\quad + \tau_{yz}(r,0)[w^{(k)}(\delta\beta-r,\pi) - w^{(k+1)}(\delta\beta-r,-\pi)]\}dr\,, \end{aligned} \tag{30}$$

where polar coordinates $(r,\phi)$ are used for the convenience of computation. The interlaminar stresses, $\sigma_y$, $\tau_{xy}$, and $\tau_{yz}$ in Eq 30, may be obtained from the crack-tip stress field equations such as Eq 27. The corresponding displacements are also those of the crack-tip field equations obtained in the previous section.

## 5. NUMERICAL EXAMPLES AND DISCUSSION

The formulation and analysis for the problem outlined in previous sections have been programmed into a solution scheme suitable for numerical computation. For the purpose of illustrating the fundamental behavior of the delamination fracture in composite laminates, graphite-epoxy systems with symmetric $(\theta/-\theta/-\theta/\theta)$ fiber orientation containing edge delamination cracks along the $\theta$ and $-\theta$ ply interface are studied. The particular material system and ply orientations are selected here because they have been previously investigated in some detail.

The composite laminate is subjected to a uniform axial extension and has a geometry shown in Fig. 1 with a width-to-thickness ratio 2b/2W and uniform ply thickness $h_i$. Delamination cracks of length $a$ are assumed to emanate from the edges of the composite. Lamina properties typical of high-modulus unidirectional graphite-epoxy composite for aircraft construction are used in the computation (Table 1). For composite laminates with the aforementioned laminate geometry and ply orientations, several geometric and material symmetry conditions may be introduced to simplify the formulation further. The problem, therefore, can be solved very conveniently and accurately.

### 5.1 Symmetry and Boundary Conditions, and Further Simplifications

The symmetric ply orientations and geometry of the composite laminate (Fig. 3) lead to the following conditions for displacements:

$$\frac{\partial u}{\partial y} = \frac{\partial w}{\partial y} = \frac{\partial v}{\partial x} = 0 \qquad \text{on } x = b-a, \tag{31a}$$

$$\frac{\partial v}{\partial x} = \frac{\partial w}{\partial y} = \frac{\partial u}{\partial y} = 0 \qquad \text{on } y = -h_2, \tag{31b}$$

where the origin of the coordinates is moved to the left tip of the delamination. The traction-free boundary conditions on edges and lateral surfaces of the composite laminate may be written as

$$\sigma_x = \tau_{xy} = \tau_{xz} = 0 \qquad \text{on } x = -a, \tag{31c}$$

$$\sigma_y = \tau_{xy} = \tau_{yz} = 0 \qquad \text{on } y = h_1. \tag{31d}$$

Thus, only a quarter of the laminate cross section needs to be considered. The boundary conditions, Eqs 31a-d, contain arbitrariness of rigid body displacements, which is a characteristic of traction boundary value problems.

Since the eigen solutions, $\sigma_i^{(h)}$, satisfy Eq 19 and interface continuity conditions Eq 20, we require that $\sigma_i^{(p)}$ satisfy these conditions also. To determine $d_k^{(\alpha)}$ uniquely for Eqs 17 and 18, we further require the particular solutions satisfy the following conditions:

$$u^{(p)} = 0 \qquad \text{on } x = b-a, \tag{32a}$$

$$v^{(p)} = 0 \qquad \text{on } y = -h_2, \tag{32b}$$

$$w^{(p)} = 0 \qquad \text{at } (0,0,0). \tag{32c}$$

Substituting Eqs 17 and 18 into Eqs 19, 20 and 32 gives

$$u_o^{(\alpha)} = -\sum_{k=1}^{3} [d_k^{(1)} p_k^{(1)} + \bar{d}_k^{(1)} \bar{p}_k^{(1)}](b - a), \qquad (\alpha=1,2) \tag{33a}$$

$$v_o^{(\alpha)} = \sum_{k=1}^{3} [d_k^{(2)} q_k^{(2)} \mu_k^{(2)} + \bar{d}_k^{(2)} \bar{q}_k^{(2)} \bar{\mu}_k^{(2)}] \, h_2, \tag{33b}$$

$$w_o^{(\alpha)} = 0, \tag{33c}$$

$$\omega_1^{(\alpha)} = \omega_2^{(\alpha)} = 0 \tag{33d}$$

$$\omega_3^{(\alpha)} = -\sum_{k=1}^{3} [d_k^{(\alpha)} q_k^{(\alpha)} + \bar{d}_k^{(\alpha)} \bar{q}_k^{(\alpha)}], \tag{33e}$$

and

$$\sum_{k=1}^{3} [d_k^{(\alpha)} + \bar{d}_k^{(\alpha)}] = -\sigma_{yo}^{(\alpha)} \tag{34a}$$

$$\sum_{k=1}^{3} [d_k^{(\alpha)} \eta_k^{(\alpha)} + \bar{d}_k^{(\alpha)} \bar{\eta}_k^{(\alpha)}] = \tau_{yzo}^{(\alpha)}, \tag{34b}$$

$$\sum_{k=1}^{3} [d_k^{(\alpha)} \mu_k^{(\alpha)} + \bar{d}_k^{(\alpha)} \bar{\mu}_k^{(\alpha)}] = \tau_{xyo}^{(\alpha)}, \tag{34c}$$

$$\sum_{k=1}^{3} [d_k^{(1)} p_k^{(1)} + \bar{d}_k^{(1)} \bar{p}_k^{(1)}] = \sum_{k=1}^{3} [d_k^{(2)} p_k^{(2)} + \bar{d}_k^{(2)} \bar{p}_k^{(2)}], \tag{34d}$$

$$\sum_{k=1}^{3} [d_k^{(1)} t_k^{(1)} + \bar{d}_k^{(1)} \bar{t}_k^{(1)}] = \sum_{k=1}^{3} [d_k^{(2)} t_k^{(2)} + \bar{d}_k^{(2)} \bar{t}_k^{(2)}], \tag{34e}$$

$$\sum_{k=1}^{3} [d_k^{(\alpha)} (q_k^{(\alpha)} + p_k^{(\alpha)} \mu_k^{(\alpha)}) + \bar{d}_k^{(\alpha)} (\bar{q}_k^{(\alpha)} + \bar{p}_k^{(\alpha)} \bar{\mu}_k^{(\alpha)})] = 0. \tag{34f}$$

Equations 34a-f give ten linear algebraic equations for twelve real unknowns for $\sigma_i^{(p)}$ and $u_i^{(p)}$. Hence, we may set

$$\mathrm{Im}[d_3^{(\alpha)}] = 0 \tag{35a}$$

to reduce the additional degrees of freedom. For symmetric angle-ply laminates, it can be shown that Eq 34f is satisfied identically.

Therefore, instead of using Eq 35a, it may be required

$$d_3^{(\alpha)} = 0. \tag{35b}$$

Since the complete solutions for stresses and displacements must satisfy the symmetry and remote boundary conditions, Eqs 31a-d, the following relations can be established immediately to evaluate $\sigma_i^{(h)}$ and $u_i^{(h)}$:

$$\sigma_i^{(h)} + \sigma_i^{(p)} = 0 \qquad (i=1,5,6) \qquad \text{on} \quad x = -a, \tag{36a}$$

$$\sigma_i^{(h)} + \sigma_i^{(p)} = 0 \qquad (i=2,4,6) \qquad \text{on} \quad y = h_1, \tag{36b}$$

and

$$\frac{\partial u^{(h)}}{\partial y} + \frac{\partial u^{(p)}}{\partial y} = 0, \quad \frac{\partial v^{(h)}}{\partial x} + \frac{\partial v^{(p)}}{\partial x} = 0, \quad \frac{\partial w^{(h)}}{\partial y} + \frac{\partial w^{(p)}}{\partial y} = 0, \quad \text{on} \quad x = b-a, \tag{36c}$$

$$\frac{\partial v^{(h)}}{\partial x} + \frac{\partial v^{(p)}}{\partial x} = 0, \quad \frac{\partial u^{(h)}}{\partial x} + \frac{\partial u^{(p)}}{\partial x} = 0, \quad \frac{\partial w^{(h)}}{\partial y} + \frac{\partial w^{(p)}}{\partial y} = 0, \quad \text{on} \quad y = -h_2. \tag{36d}$$

By using the eigenfunctions derived previously and the boundary collocation method, the boundary conditions given in Eqs 36a-d can be matched conveniently in the least-square sense. Thus, the eigen solutions for $\sigma_i^{(h)}$ and $u_i^{(h)}$ can be determined. Numerical solutions for the problem by using the collocation procedure are related to the truncation of eigenfunctions and number of collocation stations. Due to space limitation, the detailed discussion of solution convergence and accuracy is reported elsehwere [16]. The results presented in this section are from collocation calculation, which has a maximum mismatch within one percent deviation from prescribed boundary conditions.

## 5.2 Stress Singularity for Delamination in Composites

Now consider a delamination lying between $\theta$ and $-\theta$ plies (Fig. 1) in a graphite-epoxy composite with ply properties given in Table 1. The interface continuity and traction boundary conditions along crack surfaces lead to a standard eigenvalue problem for the homogeneous solution, as discussed in Section 3.3. The eigenvalues $\delta_m$ obtained from the transcendental equation provide basic structures of near-field stress and displacement solutions for the delamination problem. The order of stress singularity and the asymptotic nature of the crack tip stresses depend on the values of $\delta_m$, which satisfy the constraint condition of Eq 24. Thus, the eigenvalues corresponding to this restriction are of fundamental importance in understanding the delamination failure behavior. For edge delaminated $(\pm\theta)_s$ graphite-epoxy composites with various fiber orientations, the eigenvalues $\delta_m$, which satisfy the aforementioned constraint condition, are found by the present eigen analysis and given in Table 2. The stress singularities for an interface crack between two highly anisotropic laminae are observed to contain a pair of complex conjugates, $\delta_{1,2} = -0.5 \pm i\gamma$, and a constant, $\delta_3 = -0.5$. This situation is unique and different from that of an interface crack between two isotropic or orthotropic media in the sense that $\delta_1$, $\delta_2$ and $\delta_3$ exist simultaneously in the present delamination problem. In the degenerated cases such as $\pm\theta = 0°$ and $90°$, the composite laminates become unidirectional. The delamination is located in an orthotropic material; the classical inverse square-root singularity for crack-tip stresses is recovered fully. It is noted that the

present physical model and the eigenfunction analysis lead to an oscillatory stress singularity, as are the cases of interface cracks in isotropic or orthotropic materials.

## 5.3 Asymptotic Stress Field Around Delamination

Complete solutions for delamination cracks in finite dimensional composite laminates are obtainable by using the present Lekhnitskii's complex stress potential formulation and eigenfunction expansion. With the aid of the boundary collocation method, the asymptotic stress field around a delamination may be expressed in a general form as

$$\sigma_j = \sum_{k=1}^{3} \{(D_{jk} Z_k^{-0.5+i\gamma} + D_{j(k+3)} \bar{Z}^{-0.5+i\gamma}) + (E_{jk} Z_k^{-0.5-i\gamma} + E_{j(k+3)} \bar{Z}^{-0.5-i\gamma}) + (F_{jk} Z_k^{-0.5} + F_{j(k+3)} \bar{Z}^{-0.5})\}$$

$$(j=1,2,.....,6), \tag{37}$$

where $D_{jk}$, $E_{jk}$, and $F_{jk}$ are known quantities satisfying the following relations:

$$D_{jk} = \bar{E}_{j(k+3)}, \quad D_{j(k+3)} = \bar{E}_{jk}, \quad F_{jk} = \bar{F}_{j(k+3)}, \tag{38}$$

to insure $\sigma_j$ being real. More concisely, $\sigma_j$ can be written as

$$\sigma_j = r^{-\frac{1}{2}} [A_j \cos(\gamma \ell n\, r) + B_j \sin(\gamma \ell n\, r) + C_j]. \tag{39}$$

For illustrative purposes, the structures of near-field stresses and displacements ahead of a delamination (r,0) are given for a

(45°/-45°/-45°/45°) graphite-epoxy laminate with $h_1 = h_2 = 1$ in., $a = 1$ in. and $2b/h = 4$ subjected to $\varepsilon_z = e$ as follows:

$$\sigma_y(r,0) = [0.04339\cos(0.03434\ \ell n\ r) + 0.39498\sin(0.03434\ \ell n\ r)]\ r^{-0.5} + 0(1), \tag{40a}$$

$$\tau_{yz}(r,0) = [0.45347\ \cos(0.03434\ \ell n\ r) - 0.04981\sin(0.03434\ \ell n\ r)]\ r^{-0.5} + 0(1), \tag{40b}$$

$$\tau_{xy}(r,0) = -0.002449\ \ r^{-0.5} + 0(1)\ , \tag{40c}$$

and

$$u^{(1)}(\delta\beta - r,\pi) = \{-0.29576\cos[0.03434\ \ell n(\delta\beta - r)] + 0.01208\sin[0.03434\ \ell n(\delta\beta - r)]\}(\delta\beta - r)^{0.5} - 0.003403(\delta\beta - r)^{0.5} + 0(1), \tag{41a}$$

$$v^{(1)}(\delta\beta - r,\pi) = \{0.02888\cos[0.03434\ \ell n(\delta\beta - r)] + 0.70682\sin[0.03434\ \ell n(\delta\beta - r)]\}(\delta\beta - r)^{0.5} + 0(1), \tag{41b}$$

$$w^{(1)}(\delta\beta - r,\pi) = \{0.61564\ \cos[0.03434\ \ell n(\delta\beta - r)] - 0.025155\ \sin[0.03434\ \ell n(\delta\beta - r)]\}(\delta\beta - r)^{0.5} + 0.001602(\delta\beta - r)^{0.5} + 0(1), \tag{41c}$$

where the components of stress are scaled by $10^6 \times \varepsilon_z$, and the displacements by $\varepsilon_z$. It is noted that the elastic stresses near the

delamination crack tip in a composite laminate possesses the well known oscillatory behavior, and the displacement field also exhibits an oscillatory nature with crack surfaces overlapping each other. As first pointed out by Malyshev, et al. [7] and later by England [5] and Erdogan [8] for interfacial cracks between dissimilar isotropic media, the phenomenon of crack surface overlapping is confined to an extremely small region and the interpenetration is not of significance in practical terms of fracture mechanics. However, for certain combinations of material properties, ply orientations and loading conditions in composite laminates, the crack surface contact region has been found to be extremely large [16]. Thus the current model needs to be modified to account for the crack surface closure and contact stresses [16]. Studies on interface crack closure in dissimilar isotropic media were reported recently by Comninou [17], Atkinson [18] and Achenback [11].

## 5.4 Delamination Crack Tip Stress Intensity Factors

Since the Irwin fracture criterion is local in nature and requires precise knowledge of the local conditions at the delamination crack tip, the stress intensity solutions are obviously of great significance. According to the present fracture mechanics theory of composite delamination, stress intensity factors, $K_I$, $K_{II}$ and $K_{III}$, may be evaluated by the rigorous analysis described in Section 4. The $K_I$, $K_{II}$ and $K_{III}$ lead to detailed information of the stress and displacement fields in the neighborhood of the delamination crack tip, and may relate to the onset of delamination extension upon reaching a critical level. The

magnitudes of $K_i$ shown in the formulation depend on the delamination length, ply orientations, laminate geometry, and loading conditions.

Consider the $(\theta/-\theta/-\theta/\theta)$ graphite-epoxy composites with various fiber orientations subjected to uniform axial extension $\varepsilon_z$. For illustrative purposes, we choose a composite with a width-to-thickness ratio $2b/(2h)$ equal to 8, ply thickness $h_1 = h_2 = 1$ in., and delamination length $a = 1$ in. The mixed mode $K_I$, $K_{II}$ and $K_{III}$ are determined and given in Table 3 for various $\theta$'s. It is observed that even though the composite laminate is under the simplest loading condition, the delamination crack tip response is very complicated due to the complex interlaminar stress distribution, the nonhomogeneity of the solid, the anisotropic ply properties, and the unusual delamination configuration with respect to the loading direction. The out-of-plane tearing mode stress intensity factor $K_{III}$ caused by interlaminar shear $\tau_{yz}$ is about one or two orders of magnitude higher than $K_I$ and $K_{II}$ in general in the laminates studied. The opening mode stress intensity $K_I$ is also very significant due to the interlaminar normal stresses $\sigma_y$. The simultaneous presence of $K_I$, $K_{II}$ and $K_{III}$ in the delamination problem is unique to angle-ply fiber composites, and is not observed in fracture problems for bonded dissimilar isotropic media in general. The delamination behavior is inherently three dimensional in nature; for composites with more general laminations, crack geometry and loading conditions, fully three-dimensional stress and fracture analyses are essential for obtaining complete information.

The influence of laminate geometric variables on the delamination behavior is best illustrated by examining the changes of $K_I$, $K_{II}$ and

$K_{III}$ with the relative thickness of upper and lower plies $h_1/h_2$ in a (45°/-45°/-45°/45°) graphite-epoxy composite (with $h_1 + h_2 = W = 2$ in.). Given the crack length, ($a$ = 1 in.), laminate dimensions (2b = 4 in.), and the loading condition as previously, the delamination stress intensities for various $h_1/h_2$'s are shown in Fig. 4. The crack tip tearing and opening stresses $\tau_{yz}$ and $\sigma_y$ have a maximum intensification as the ply thicknesses $h_i$ become identical, i.e., $h_1/h_2 = 1$. The $K_{II}$, however, reaches a minimum due to the reduction of $\tau_{xy}$. It should be noted here that the $K_I$, $K_{II}$ and $K_{III}$ depend on material constants of all plies as well as the overall geometry. Therefore, the dependency of $K_i$ on ply properties is not a simple matter of identifying them with geometric variables, and they may not have the simple physical interpretation as in the homogeneous case.

## 5.5 Strain Energy Release Rates for Delamination

The equilibrium and stability of delamination are commonly examined from an energy rate point of view. The strain energy release rate G defined in Eq 30 is a quantity characterizing the driving force for delamination extension. The delamination-growth driving force can be easily determined after the establishment of the local asymptotic stress and displacement fields. For the edge delamination problem in graphite-epoxy composites considered here, the G value may be obtained in a general form as

$$G = G_I + G_{II} + G_{III}$$

$$= \lim_{\delta\beta\to 0} \frac{1}{2\delta\beta} \int_0^{\delta\beta} \{A_1 \cos[\gamma \ln(\frac{\delta\beta - r}{r})] + A_2 \sin[\gamma \ln(\frac{\delta\beta - r}{r})] + A_3\} (\frac{\delta\beta - r}{r})^{0.5} dr, \quad (42)$$

where $\gamma = \mathrm{Im}[\delta_1]$. Equation 42 has the form similar to the one derived previously for an elastic-half space problem by Willis [19]. The singular integration may be carried out by defining an anlytical function with the cut $0 \le x \le \delta\beta$

$$f(z) = \left(\frac{z - \delta\beta}{z}\right)^{0.5+i\gamma} \tag{43a}$$

so that we have

$$\int_0^{\delta\beta} \left(\frac{\delta\beta - r}{r}\right)^{0.5} \cos\left[\gamma \ln\left(\frac{\delta\beta - r}{r}\right)\right] dr = \pi\delta\beta/(e^{-\gamma\pi} + e^{\gamma\pi}), \tag{43b}$$

$$\int_0^{\delta\beta} \left(\frac{\delta\beta - r}{r}\right)^{0.5} \sin\left[\gamma \ln\left(\frac{\delta\beta - r}{r}\right)\right] dr = 2\,\gamma\pi\delta\beta/(e^{-\gamma\pi} + e^{\gamma\pi}). \tag{43c}$$

Thus, the total energy release rate G can be determined immediately by substituting Eq 43 into Eq 42. Table 4 shows the change of G values with ply orientations for the $(\theta/-\theta/-\theta/\theta)$ graphite-epoxy composites with the material properties in Table 1.

To study the basic nature of delamination extension in angle-ply composites, strain energy release rates in the $(45°/-45°/-45°/45°)$ graphite-epoxy with various crack lengths are examined. Effects of laminate width on delamination crack extension is also investigated. The change of total strain energy release rate G with delamination length $a$ is given in Fig. 5 to illustrate fundamental characteristics of the delamination fracture. For the composite laminates with various 2b/2h's, the G is observed to change with delamination length in a unique manner. The maximum energy release rate or crack extension driving force occurs at a delamination length approximately equal to one or two ply thicknesses in the composite studied, depending on the (2b/2h) ratio. As

the delamination exceeds this characteristic dimension, G decreases monotonically.

On the basis of fracture mechanics, several important features regarding delamination fracture are revealed from the Figure. Assuming that the material resistance to delamination growth remains constant (i.e., the failure criterion, $G_c$ = constant, is used), we can immediately conclude that there exists a critical delamination length associated with the maximum G (for example, $a^* \simeq 2h$ for the case b/h = 8) for each composite laminate; the word "critical" means the one that experiences stable crack extension at the lowest load. It also indicates that any interlaminar edge flaw $a_o$ inherently in the composite, which is less than $a^*$, will experience rapidly unstable growth as the load or G reaches a critical level, and is anticipated to be arrested at a later stage. Any initial delamination greater than $a^*$ will experience a stable growth under monotonically rising loads; that is, there exists an inherently built-in crack arrest mechanism for edge delamination. These phenomena predicted by the G - $a$ curve have been noted by several researchers conducting experimental and analytical studies on the delamination fracture. The $a^*$ may be an important quantity in the life prediction for delaminated composite materials and structures subjected to static and cyclic loading.

The delamination strain energy release rate is also a function of other geometric variables. For example, G is significantly affected by the relative ply thickness $h_1/h_2$. In a (45°/-45°/-45°/45°) graphite-epoxy with a geometry given before, the change of G with $h_1/h_2$ is given

in Fig. 6, where maximum driving force occurs at $h_1 = h_2$ indicating the criticality of the relative ply thickness to delamination fracture in composites.

It is noted here that, even though the near-field stresses possess an oscillatory singularity and $K_i$ may not have the usual significance attached to them as in the cohesive (homogeneous) case, the energy release rate G is well defined mathematically and physically, and should be the quantity of major interest. The G and its components $G_I$, $G_{II}$ and $G_{III}$ can be evaluated theoretically and experimentally to provide a basic measure of the delamination fracture.

## 6. SUMMARY AND CONCLUSIONS

An analytical method for studying delamination is presented in this paper. Fundamental nature of edge delamination in advanced fiber composite laminates is examined. Based on the theory of anisotropic elasticity, the composite delamination problem is formulated by using Lekhnitskii's complex-variable stress potentials and an eigenfunction expansion method. Exact orders of the three-dimensional stress singularity in a delamination crack tip region are determined from the eigen analysis. With the aid of a boundary collocation technique, complete stress and displacement fields in a finite-dimensional, delaminated composite are fully determined. Fracture mechanics parameters such as the mixed-mode stress intensity factors and associated energy release rates for edge delamination are calculated explicitly. Solutions are obtained for edge-delaminated $(\theta/-\theta/-\theta/\theta)$ angle-ply composites under uniform axial extension. Effects of delamination lengths, fiber orientations, lamination and geometric variables are studied in detail.

Based on the information given in the previous sections, the following conclusions may be drawn:

1. An analytical method based on the theory of anisotropic elasticity is successfully developed to study edge delamination in angle-ply composite laminates. Formulation of the problem is carried out by using Lekhnitskii's complex stress functions. Stress singularities for delamination between highly anisotropic laminae are obtainable by using an eigenfunction analysis. The order of delamination crack-tip

stress singularity is different from that of an interface crack between dissimilar isotropic or orthotropic media by the simultaneous presence of three characteristic eigenvalues of $-0.5+i\gamma$, $-0.5-i\gamma$, and $-0.5$.

3. The fracture mechanics concept may be extended to delamination problems in anisotropic composite laminates by properly defining the interlaminar crack-tip stress intensity factors such as Eqs 29a-c and strain energy release rates. For angle-ply composite laminates, $K_I$, $K_{II}$ and $K_{III}$ always occur simultaneously for an edge delamination with $K_{III}$ being one or two orders of magnitude higher than the other two.
4. Complete stress and displacement fields in a delaminated composite may be accurately determined by a combined eigenfunction expansion and a boundary collocation method. The asymptotic solutions are characterized by $K_i$ (i=I,II,III) and possess the well known oscillatory behavior. The crack surface overlapping could be very large in some composite systems with certain combinations of fiber orientations, ply stacking sequences, and loading conditions; modifications [16] of the current model to include crack closure may be needed for these cases.
5. The crack extension driving force or strain energy release rate for edge delamination in composite laminates can be accurately determined by using Irwin's crack extension concept. Delamination stability in composite laminates

under monotonically rising loads can be assessed for any inherent interlaminar flaw relative to the critical delamination size $a^*$ obtained in the current G - $a$ curve.

## 7. ACKNOWLEDGMENT

The work described in this paper was supported in part by the National Aeronautics and Space Administration-Lewis Research Center (NASA-LRC), Cleveland, Ohio under Grant NSG 3044. The author is grateful to Dr. C. C. Chamis of NASA-LRC, Dr. G. P. Sendeckyj of the Air Force Flight Dynamics Laboratory, Professor A. S. D. Wang of Drexel University, and Professor H. T. Corten of the University of Illinois at Urbana-Champaign for their valuable discussion and encouragement during the course of this study.

## 8. REFERENCES


[1] Williams, M. L., "The Stresses Around a Fault or Crack in Dissimilar Media," *Bulletin of the Seismological Society of America*, Vol. 49, 1959, pp. 199-204.

[2] Zak, A. R. and William, M. L., "Crack Point Stress Singularities at a Bi-Material Interface," *Journal of Applied Mechanics*, Vol. 30, Trans. ASME, 1963, pp. 142-143.

[3] Sih, G. C. and Rice, J. R., "The Bending of Plates of Dissimilar Materials with Cracks," *Journal of Applied Mechanics*, Vol. 31, Trans. ASME, 1964, pp. 477-482.

[4] Erdogan, F., "Stress Distributions in Bonded Dissimilar Materials with Cracks," *Journal of Applied Mechanics*, Vol. 87, Trans. ASME, 1965, pp. 403-410.

[5] England, A. H., "A Crack between Dissimilar Media," *Journal of Applied Mechanics*, Vol. 87, Trans. ASME, 1965, pp. 400-402.

[6] Rice, J. R., "Plane Problems of Cracks in Dissimilar Media," *Journal of Applied Mechanics*, Vol. 87, Trans. ASME, 1965, pp. 418-423.

[7] Malyshev, B. M. and Salganik, R. L., "The Strength of Adhesive Joints Using Theory of Fracture," *International Journal of Fracture Mechanics*, Vol. 1, 1965, pp. 114-128.

[8] Erdogan, F. and Gupta, G., "The Stress Analysis of Multilayered Composites with a Flaw," *International Journal of Solids and Structures*, Vol. 7, 1971, pp. 39-61.

[9] Erdogan, F. and Gupta, G., "Layered Composite with an Interfacial Flaw," *International Journal of Solids and Structures*, Vol. 7, 1971, pp. 1089-1107.

[10] Comninou, M., "The Interface Crack," *Journal of Applied Mechanics*, Vol. 44, Trans. ASME, 1977, pp. 631-636.

[11] Achenbach, J. D., Keer, L. M. and Chen, S. H., "Loss of Adhesion at the Tip of an Interface Crack," *Journal of Elasticity*, Vol. 9, 1979, pp. 397-424.

[12] Mak, A. F., et al., "A No-Slip Interface Crack," *Journal of Applied Mechanics*, Vol. 47, Trans. ASME, 1980, pp. 347-350.

[13] Lekhnitskii, S. G., *Theory of Elasticity of an Anisotropic Body*, Holden-Day, San Francisco, CA, 1963.

[14] Wang, S. S. and Choi, I., "Delamination of Fiber Reinforced Composite Laminates,"NASA Contract Report, NASA-Lewis Research Center, Cleveland, OH, in preparation, 1981.

[15] Irwin, G. R., "Analysis of Stresses and Strains Near the End of a Crack Transversing a Plate," *Journal of Applied Mechanics*, Vol. 24, Trans. ASME, 1957, pp. 361-364.

[16] Wang, S. S. and Choi, I., "Interlaminar Cracks in Composite Laminates Subjected to Mixed-Mode Loading," ONR Contract Report, in preparation. 1981.

[17] Comninou, M., "The Interface Crack in a Shear Field," *Journal of Applied Mechanics*, Vol. 45, Trans. ASME, 1978, pp. 287-290.

[18] Atkinson, C., "On Stress Singularities and Interfaces in Linear Elastic Fracture Mechanics," *International Journal of Fracture*, Vol. 13, No. 6, 1977, pp. 807-820.

[19] Willis, J. R., "Fracture Mechanics of Interfacial Cracks," *Journal of Mechanics and Physics of Solids*, Vol. 19, 1971, pp. 353-368.

TABLE 1

Material's Constants for Graphite/Epoxy Composite Lamina

$$E_L = 20.0 \times 10^6 \text{ psi}$$

$$E_T = 2.1 \times 10^6 \text{ psi}$$

$$G_{LT} = G_{Lz} = G_{Tz} = 0.85 \times 10^6 \text{ psi}$$

$$\nu_{LT} = \nu_{Lz} = \nu_{Tz} = 0.21$$

TABLE 2

Dominant Stress Singularities for Delamination in $(\theta/-\theta/-\theta/\theta)$ Graphite-Epoxy Composites

| $\theta$ | $\delta_{1,2}$ | $\delta_3$ |
|---|---|---|
| 0° | - 0.5 | - 0.5 |
| 15° | - 0.5 ± 0.00642i | - 0.5 |
| 30° | - 0.5 ± 0.02399i | - 0.5 |
| 45° | - 0.5 ± 0.03434i | - 0.5 |
| 60° | - 0.5 ± 0.02942i | - 0.5 |
| 75° | - 0.5 ± 0.01579i | - 0.5 |
| 90° | - 0.5 | - 0.5 |

TABLE 3

Stress Intensity Factors $K_i$* for Edge Delamination in (θ/-θ/-θ/θ) Angle-Ply Graphite-Epoxy Composite† Subjected to Uniform Axial Strain

| ±θ | $K_I$ | $K_{II}$†† | $K_{III}$†† |
|---|---|---|---|
| 15° | 0.08645 | 0.01214 | -4.5588 |
| 30° | 0.2330 | 0.03330 | -3.6604 |
| 45° | 0.1347 | 0.01380 | -1.2968 |
| 60° | 0.02025 | 0.001360 | -0.1775 |
| 75° | 0.006268 | -0.0002948 | 0.0818 |

*$K_i$ (psi - $\sqrt{\text{in.}}$) are scaled by $10^6$ $\varepsilon_z$

†$a = h_1 = h_2 = 1$ in., $b = 8$ in.

††For the delamination crack in the first quadrant

TABLE 4

Energy Release Rate G for Edge Delamination in $(\theta/-\theta/-\theta/\theta)$ Angle-Ply Graphite-Epoxy Composite† Under Uniaxial Extension $\varepsilon_z$

| $\pm\theta$ | $G/10^6\ \varepsilon_z^2$ (psi-in.) |
|---|---|
| 15° | 8.1076 |
| 30° | 4.0506 |
| 45° | 0.5740 |
| 60° | 0.0138 |
| 75° | 0.0036 |

†$a = h_1 = h_2$ 1 in., b = 8 in.

LIST OF FIGURE CAPTIONS

Fig. 1 Edge Delamination Geometry and Coordinate System for Symmetric Angle-Ply Composite Laminate

Fig. 2 Edge Delamination between $k$th and $(k+1)$th plies

Fig. 3 Symmetry and Boundary Conditions for $(\theta/-\theta/-\theta/\theta)$ Graphite-Epoxy Composite

Fig. 4 Stress Intensity Factors, $K_I$, $K_{II}$ and $K_{III}$, of an Edge Delamination Crack in $(45°/-45°/-45°/45°)$ Graphite-Epoxy Composite with Various Ply-Thickness Ratios $h_1/h_2$

Fig. 5 Strain Energy Release Rate G vs Delamination Crack Length $a$ in $(45°/-45°/-45°/45°)$ Graphite-Epoxy Composites with Various Laminate Widths b's ($h_1 = h_2 = 1$ in.)

Fig. 6 Effect of Relative Ply Thickness $h_1/h_2$ on Strain Energy Release Rate G in $(45°/-45°/-45°/45°)$ Graphite-Epoxy Composites ($a = 1$ in., $W = 2$ in., $2b = 4$ in.)

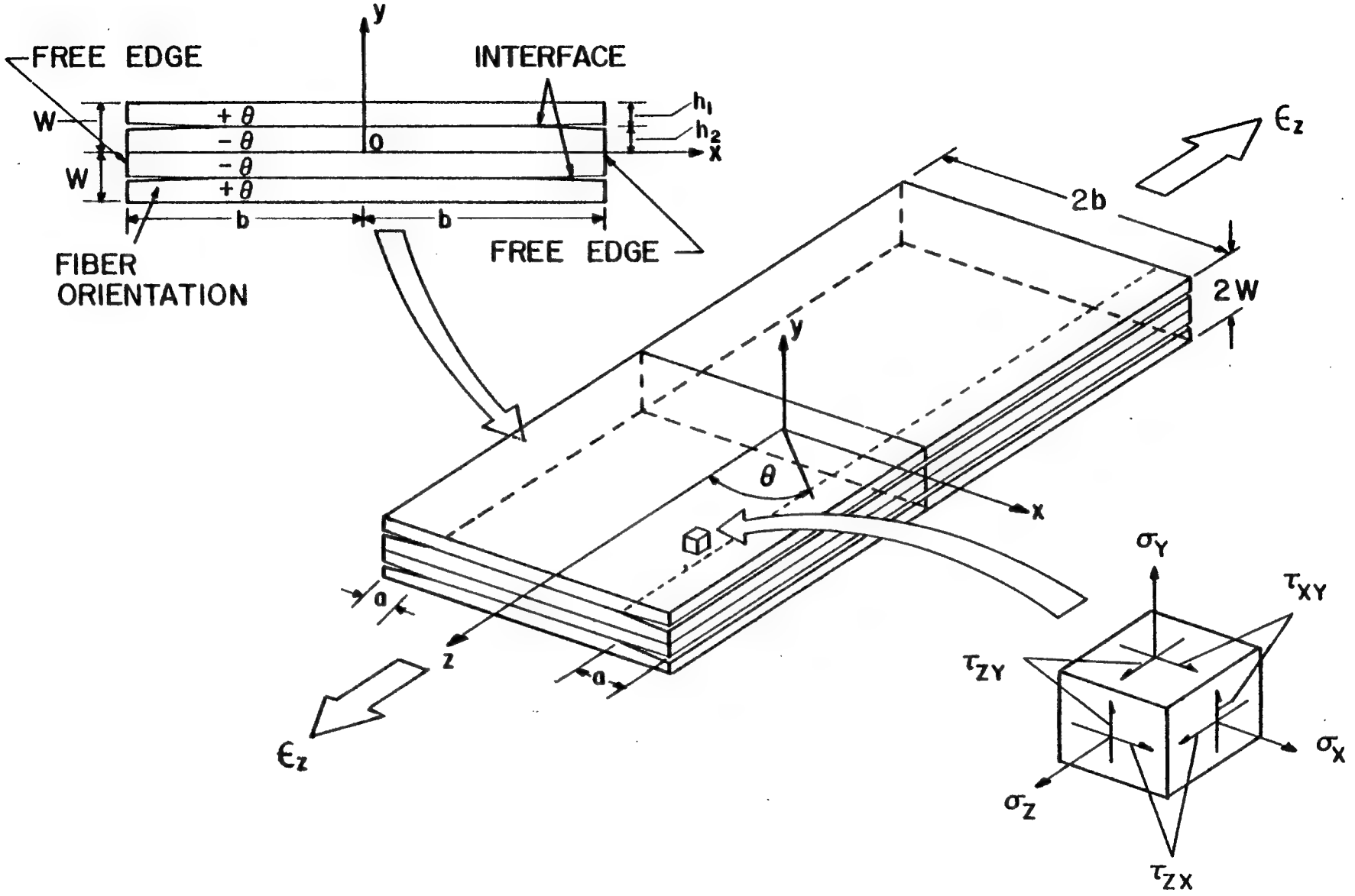


FIG. 1 EDGE DELAMINATION GEOMETRY AND LAMINATE CONFIGURATION.

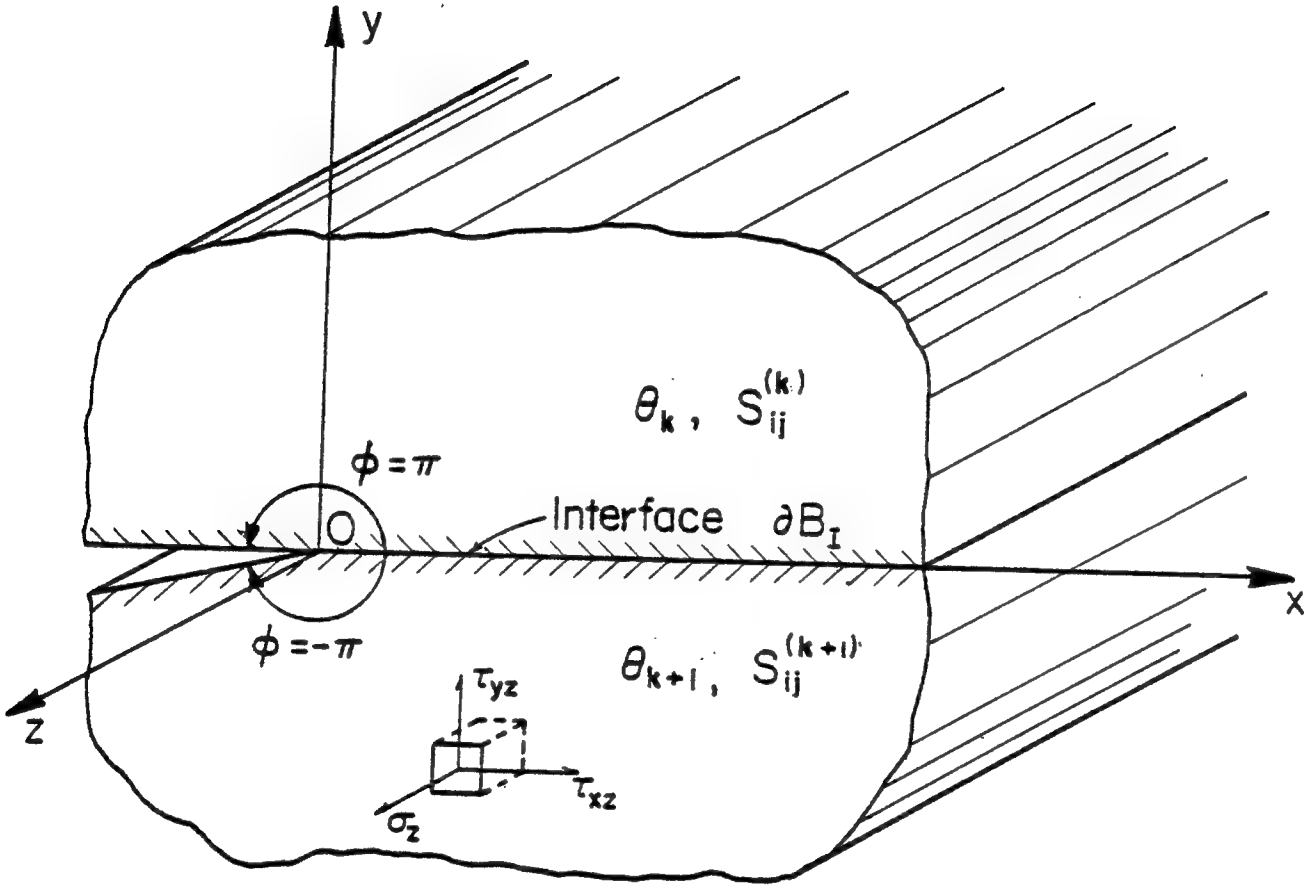


FIG. 2

EDGE DELAMINATION BETWEEN kTH AND (k+1)TH PLIES

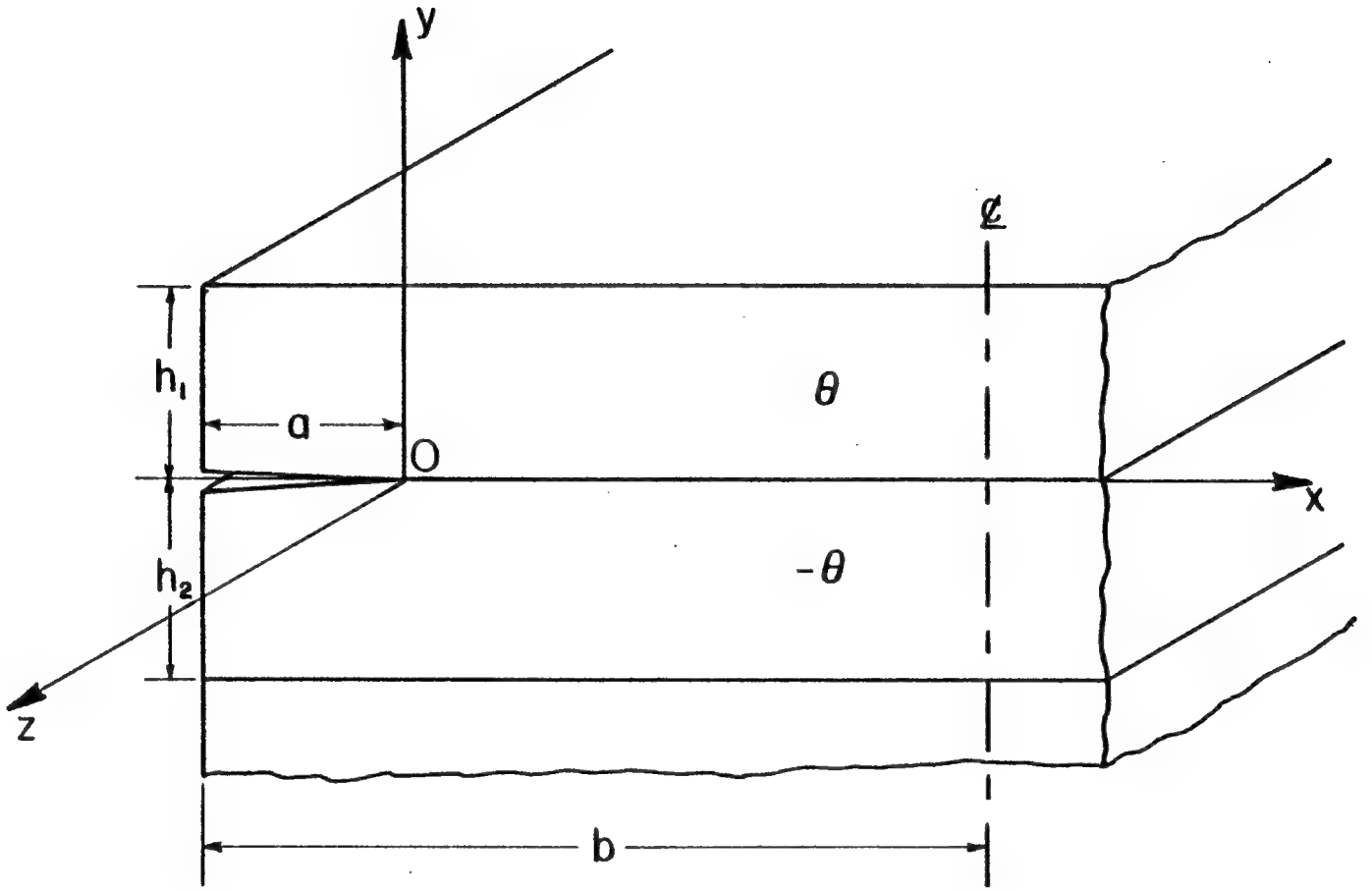


FIG. 3

SYMMETRY AND BOUNDARY CONDITIONS FOR (θ/-θ/-θ/θ) GRAPHITE-EPOXY COMPOSITE

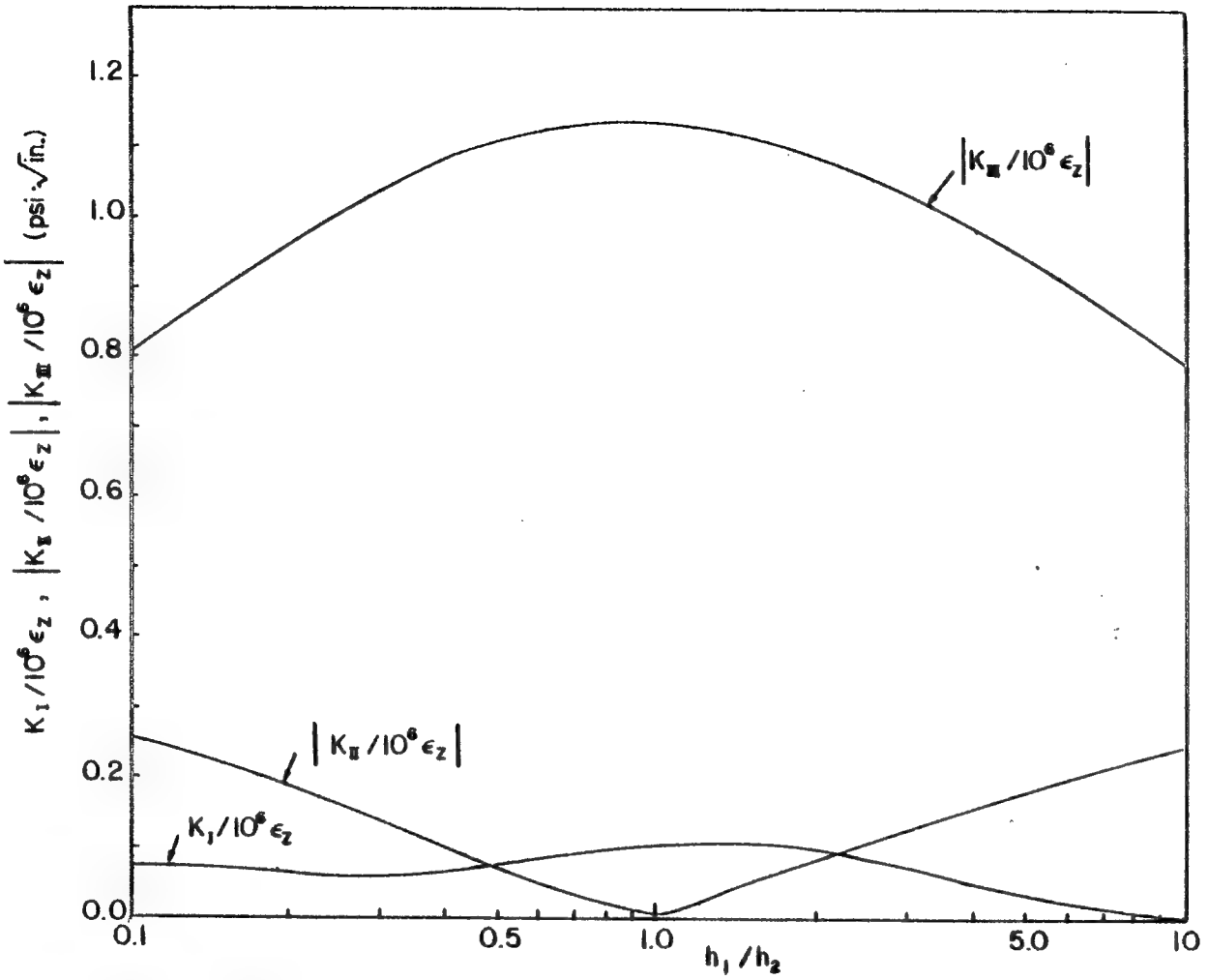


FIG. 4 STRESS INTENSITY FACTORS, $K_I$, $K_{II}$, AND $K_{III}$, OF EDGE DELAMINATION CRACK IN (45°/-45°/-45°/45°) GRAPHITE/EPOXY COMPOSITES WITH VARIOUS PLY THICKNESS RATIO $h_1/h_2$.

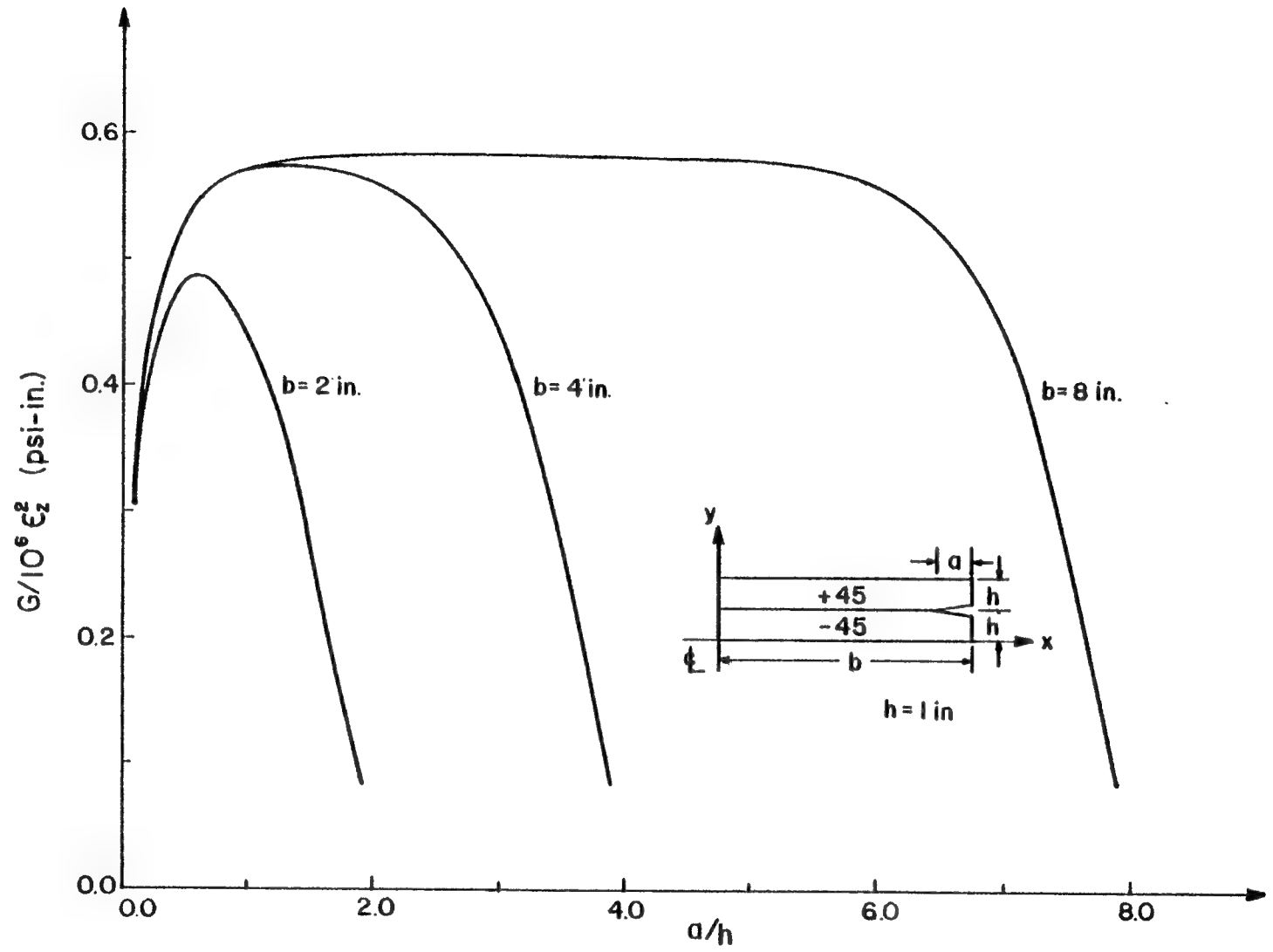


FIG. 5

STRAIN ENERGY RELEASE RATE $G$ vs DELAMINATION CRACK LENGTH $a$ IN (45°/-45°/-45°/45°) GRAPHITE-EPOXY COMPOSITES WITH VARIOUS LAMINATE WIDTHS $b$'s ($h_1 = h_2 = 1$ in.)

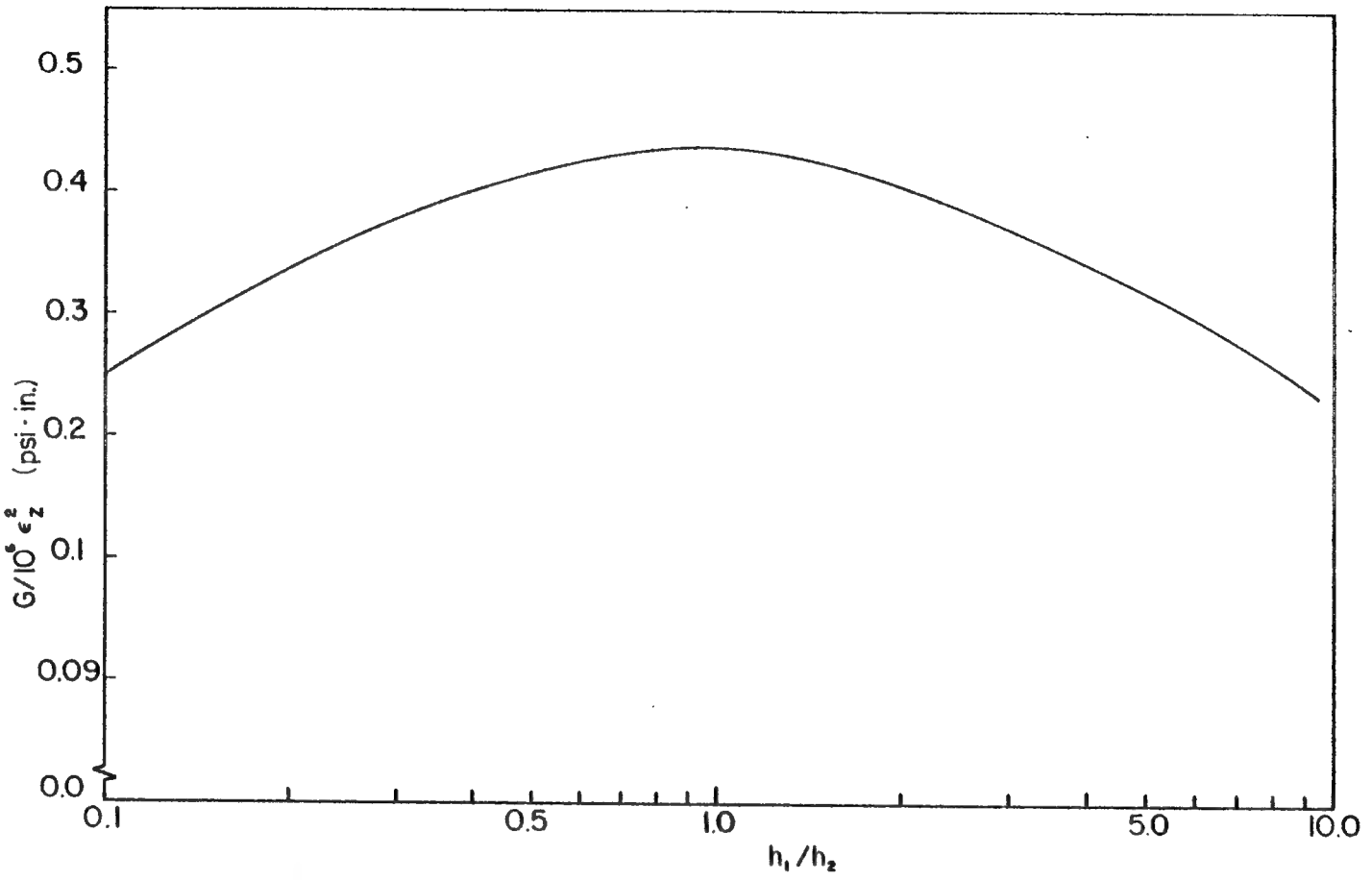


FIG. 6 ENERGY RELEASE RATE G FOR EDGE DELAMINATION CRACK IN (45°/-45°/-45°/45°) GRAPHITE/EPOXY COMPOSITES WITH VARIOUS PLY THICKNESS RATIO $h_1/h_2$.

## APPENDIX 1

### Materials Parameters for Delamination Crack-Tip Eigenvalues in Cross-Ply Composite Laminate

$$\delta_n = n \qquad \text{or}$$

$$\delta_n = (n - \tfrac{1}{2}) \pm \frac{i}{2\pi} \ln\{[b + (b^2 - 4a^2)^{\frac{1}{2}}]/(2a)\}$$

where

$$a = -M_1^{(k)} M_2^{(k+1)} - M_2^{(k)} M_1^{(k+1)} + M_3^{(k)} M_3^{(k+1)} + \bar{M}_3^{(k)} \bar{M}_3^{(k+1)} + M_4^{(k)} + M_4^{(k+1)},$$

$$b = -2M_1^{(k)} M_2^{(k)} + M_3^{(k)} M_3^{(k)} + \bar{M}_3^{(k)} \bar{M}_3^{(k)} - 2M_1^{(k)} M_2^{(k+1)} - 2M_2^{(k)} M_1^{(k+1)} - 2\bar{M}_3^{(k)} M_3^{(k+1)} - 2M_3^{(k)} \bar{M}_3^{(k+1)} - 2M_1^{(k+1)} M_2^{(k+1)} + M_3^{(k+1)} M_3^{(k+1)} + \bar{M}_3^{(k+1)} \bar{M}_3^{(k+1)},$$

and

$$M_1^{(\alpha)} = \frac{1}{2} \tilde{S}_{11}^{(\alpha)} \{(\mu_1^{(\alpha)} + \mu_2^{(\alpha)}) - (\bar{\mu}_1^{(\alpha)} + \bar{\mu}_2^{(\alpha)})\},$$

$$M_2^{(\alpha)} = \frac{1}{2} \tilde{S}_{11}^{(\alpha)} \{\mu_1^{(\alpha)} \mu_2^{(\alpha)} (\bar{\mu}_1^{(\alpha)} + \bar{\mu}_2^{(\alpha)}) - \bar{\mu}_1^{(\alpha)} \bar{\mu}_2^{(\alpha)} (\mu_1^{(\alpha)} + \mu_2^{(\alpha)})\},$$

$$M_3^{(\alpha)} = \tilde{S}_{11}^{(\alpha)} \mu_1^{(\alpha)} \mu_2^{(\alpha)} - \tilde{S}_{12}^{(\alpha)}$$

$$M_4^{(\alpha)} = -\tilde{S}_{11}^{(\alpha)} \tilde{S}_{22}^{(\alpha)} - (\tilde{S}_{12}^{(\alpha)})^2 + \tilde{S}_{11}^{(\alpha)} (\mu_1^{(\alpha)} \mu_2^{(\alpha)} + \bar{\mu}_1^{(\alpha)} \bar{\mu}_2^{(\alpha)}) [\tilde{S}_{12}^{(\alpha)} - \frac{1}{2} \tilde{S}_{11}^{(\alpha)} (\mu_1^{(\alpha)} + \mu_2^{(\alpha)}) (\bar{\mu}_1^{(\alpha)} + \bar{\mu}_2^{(\alpha)})].$$

FINAL REPORT PART V - DISTRIBUTION LIST

NSG 3044

EDGE DELAMINATION IN ANGLE-PLY COMPOSITE LAMINATES

NASA CR 165439

Advanced Research Projects Agency
Washington DC 20525
Attn: Library

Advanced Technology Center, Inc.
LTV Aerospace Corporation
P.O. Box 6144
Dallas, TX 75222
Attn: D. H. Petersen
W. J. Renton

Air Force Flight Dynamics Laboratory
Wright-Patterson Air Force Base, OH 45433
Attn: E. E. Baily
G. P. Sendeckyj (FBC)
R. S. Sandhu

Air Force Materials Laboratory
Wright-Patterson Air Force Base, OH 45433
Attn: H. S. Schwartz (LN)
T. J. Reinhart (MBC)
G. P. Peterson (LC)
E. J. Morrisey (LAE)
S. W. Tsai (MBM)
N. J. Pagano
J. M. Whitney (MBM)

Air Force Office of Scientific Research
Washington DC 20333
Attn: J. F. Masi (SREP)

Air Force Office of Scientific Research
1400 Wilson Blvd.
Arlington, VA 22209

AFOSR/NA
Bolling AFB, DC 20332
Attn: A. K. Amos

Air Force Rocket Propulsion Laboratory
Edwards, CA 93523
Attn: Library

Babcock & Wilcox Company
Advanced Composites Department
P.O. Box 419
Alliance, Ohio 44601
Attn: P. M. Leopold

Bell Helicopter Company
P.O. Box 482
Ft. Worth, TX 76101
Attn: H. Zinberg

The Boeing Company
P. O. Box 3999
Seattle, WA 98124
Attn: J. T. Hoggatt, MS. 88-33
T. R. Porter

The Boeing Company
Vertol Division
Morton, PA 19070
Attn: E. C. Durchlaub

Battelle Memorial Institute
Columbus Laboratories
505 King Avenue
Columbus, OH 43201
Attn: L. E. Hulbert

Bendix Advanced Technology Center
9140 Old Annapolis Rd/Md. 108
Columbia, MD 21045
Attn: O. Hayden Griffin

Brunswick Corporation
Defense Products Division
P. O. Box 4594
43000 Industrial Avenue
Lincoln, NE 68504
Attn: R. Morse

Celanese Research Company
86 Morris Ave.
Summit, NJ 07901
Attn: H. S. Kliger

Commander
Natick Laboratories
U. S. Army
Natick, MA 01762
Attn: Library

Commander
Naval Air Systems Command
U. S. Navy Department
Washington DC 20360
Attn: M. Stander, AIR-43032D

Commander
Naval Ordnance Systems Command
U.S. Navy Department
Washington DC 20360
Attn: B. Drimmer, ORD-033
M. Kinna, ORD-033A

Cornell University
Dept. Theoretical & Applied Mech.
Thurston Hall
Ithaca, NY 14853
Attn: S. L. Phoenix

Defense Metals Information Center
Battelle Memorial Institute
Columbus Laboratories
505 King Avenue
Columbus, OH 43201

Department of the Army
U.S. Army Aviation Materials Laboratory
Ft. Eustis, VA 23604
Attn: I. E. Figge, Sr.
Library

Department of the Army
U.S. Army Aviation Systems Command
P.O. Box 209
St. Louis, MO 63166
Attn: R. Vollmer, AMSAV-A-UE

Department of the Army
Plastics Technical Evaluation Center
Picatinny Arsenal
Dover, NJ 07801
Attn: H. E. Pebly, Jr.

Department of the Army
Watervliet Arsenal
Watervliet, NY 12189
Attn: G. D'Andrea

Department of the Army
Watertown Arsenal
Watertown, MA 02172
Attn: A. Thomas

Department of the Army
Redstone Arsenal
Huntsville, AL 35809
Attn: R. J. Thompson, AMSMI-RSS

Department of the Navy
Naval Ordnance Laboratory
White Oak
Silver Spring, MD 20910
Attn: R. Simon

Department of the Navy
U.S. Naval Ship R&D Laboratory
Annapolis, MD 21402
Attn: C. Hersner, Code 2724

Director
Deep Submergence Systems Project
6900 Wisconsin Avenue
Washington DC 20015
Attn: H. Bernstein, DSSP-221

Director
Naval Research Laboratory
Washington DC 20390
Attn: Code 8430
I. Wolock, Code 8433

Drexel University
32nd and Chestnut Streets
Philadelphia, PA 19104
Attn: P. C. Chou

E. I. DuPont DeNemours & Co.
DuPont Experimental Station
Wilmington, DE 19898
Attn: D. L. G. Sturgeon

Fiber Science, Inc.
245 East 157 Street
Gardena, CA 90248
Attn: E. Dunahoo

General Dynamics
P.O. Box 748
Ft. Worth, TX 76100
Attn: D. J. Wilkins
Library

General Dynamics/Convair
P.O. Box 1128
San Diego, CA 92112
Attn: J. L. Christian
R. Adsit

General Electric Co.
Evendale, OH 45215
Attn: C. Stotler
R. Ravenhall

General Motors Corporation
Detroit Diesel-Allison Division
Indianapolis, IN 46244
Attn: M. Herman

Georgia Institute of Technology
School of Aerospace Engineering
Atlanta, GA 30332
Attn: L. W. Rehfield

Grumman Aerospace Corporation
Bethpage, Long Island, NY 11714
Attn: S. Dastin
J. B. Whiteside

Hamilton Standard Division
United Aircraft Corporation
Windsor Locks, CT 06096
Attn: W. A. Percival

Hercules, Inc.
Allegheny Ballistics Laboratory
P. O. Box 210
Cumberland, MD 21053
Attn: A. A. Vicario

Hughes Aircraft Company
Culver City, CA 90230
Attn: A. Knoell

Illinois Institute of Technology
10 West 32 Street
Chicago, IL 60616
Attn: L. J. Broutman

IIT Research Institute
10 West 35 Street
Chicago, IL 60616
Attn: I. M. Daniel

Jet Propulsion Laboratory
4800 Oak Grove Drive
Pasadena, CA 91103
Attn: Library

Lawrence Livermore Laboratory
P.O. Box 808, L-421
Livermore, CA 94550
Attn: T. T. Chiao
E. M. Wu

Lehigh University
Institute of Fracture &
Solid Mechanics
Bethlehem, PA 18015
Attn: G. C. Sih

Lockheed-Georgia Co.
Advanced Composites Information Center
Dept. 72-14, Zone 402
Marietta, GA 30060
Attn: T. M. Hsu

Lockheed Missiles and Space Co.
P.O. Box 504
Sunnyvale, CA 94087
Attn: R. W. Fenn

Lockheed-California
Burbank, CA 91503
Attn: J. T. Ryder
K. N. Lauraitis
J. C. Ekvall

McDonnell Douglas Aircraft Corporation
P.O. Box 516
Lambert Field, MS 63166
Attn: J. C. Watson

McDonnell Douglas Aircraft Corporation
3855 Lakewood Blvd.
Long Beach, CA 90810
Attn: L. B. Greszczuk

Material Sciences Corporation
1777 Walton Road
Blue Bell, PA 19422
Attn: B. W. Rosen

Massachusetts Institute of Technology
Cambridge, MA 02139
Attn: F. J. McGarry
J. F. Mandell
J. W. Mar

NASA-Ames Research Center
Moffett Field, CA 94035
Attn: Dr. J. Parker
Library

NASA-Flight Research Center
P.O. Box 273
Edwards, CA 93523
Attn: Library

NASA-George C. Marshall Space Flight Center
Huntsville, AL 35812
Attn: C. E. Cataldo, S&E-ASTN-MX
Library

NASA-Goddard Space Flight Center
Greenbelt, MD 20771
Attn: Library

NASA-Langley Research Center
Hampton, VA 23365
Attn: J. H. Starnes
J. G. Davis, Jr.
M. C. Card
J. R. Davidson

NASA-Lewis Research Center
21000 Brookpark Road, Cleveland, OH 44135

Attn: Contracting Officer, MS 501-11
Tech. Report Control, MS 5-5
Tech. Utilization, MS 3-16
AFSC Liaison, MS 501-3
S&MTD Contract Files, MS 49-6
L. Berke, MS 49-6
N. T. Saunders, MS 49-1
R. F. Lark, MS 49-6
J. A. Ziemianski, MS 49-6
R. H. Johns, MS 49-6
C. C. Chamis, MS 49-6 (8 copies)
R. L. Thompson, MS 49-6
T. T. Serafini, MS 49-1
Library, MS 60-3 (2 copies)

NASA-Lyndon B. Johnson Space Center
Houston, TX 77001
Attn: S. Glorioso, SMD-ES52
Library

NASA Scientific and Tech. Information Facility
P.O. Box 8757
Balt/Wash International Airport, MD 21240
Attn: Acquisitions Branch (15 copies)

National Aeronautics & SpaceAdministration
Office of Advanced Research & Technology
Washington DC 20546
Attn: L. Harris, Code RTM-6
M. Greenfield, Code RTM-6
D. J. Weidman, Code RTM-6

National Aeronautics & Space Administration
Office of Technology Utilization
Washington DC 20546

National Bureau of Standards
Eng. Mech. Section
Washington DC 20234
Attn: R. Mitchell

National Science Foundation
Engineering Division
1800 G. Street, NW
Washington DC 20540
Attn: Library

Northrop Corporation Aircraft Group
3901 West Broadway
Hawthorne, CA 90250
Attn: R. M. Verette
G. C. Grimes

Pratt & Whitney Aircraft
East Hartford, CT 06108
Attn: J. M. Woodward

Raytheon Co., Missile System Division
Mechanical Systems Laboratory
Bedford, MA
Attn: P. R. Digiovanni

Rensselaer Polytechnic Institute
Troy, NY 12181
Attn: R. Loewy

Rockwell International
Los Angeles Division
International Airport
Los Angles, CA 90009
Attn: L. M. Lackman
D. Y. Konishi

Sikorsky Aircraft Division
United Aircraft Corporation
Stratford, CT 06602
Attn: Library

Southern Methodist University
Dallas, TX 75275
Attn: R. M. Jones

Space & Missile Systems Organization
Air Force Unit Post Office
Los Angeles, CA 90045
Attn: Technical Data Center

Structural Composites Industries, Inc.
6344 N. Irwindale Avenue
Azusa, CA 91702
Attn: R. Gordon

Texas A&M
Mechanics & Materials Research Center
College Station, TX 77843
Attn: R. A. Schapery
Y. Weitsman

TRW, Inc.
23555 Euclid Avenue
Cleveland, OH 44117
Attn: I. J. Toth

Union Carbide Corporation
P. O. Box 6116
Cleveland, OH 44101
Attn: J. C. Bowman

United Technologies Research Center
East Hartford, CT 06108
Attn: R. C. Novak
Dr. A. Dennis

University of Dayton Research Institute
Dayton, OH 45409
Attn: R. W. Kim

University of Delaware
Mechanical & Aerospace Engineering
Newark, DE 19711
Attn: B. R. Pipes

University of Illinois
Department of Theoretical & Applied Mechanics
Urbana, IL 61801
Attn: S. S. Wang

University of Oklahoma
School of Aerospace Mechanical & Nuclear Engineering
Norman, OK 73069
Attn: C. W. Bert

University of Wyoming
College of Engineering
University Station Box 3295
Laramie, WY 82071
Attn: D. F. Adams

U. S. Army Materials & Mechanics Research Center
Watertown Arsenal
Watertown, MA 02172
Attn: E. M. Lenoe
D. W. Oplinger

V.P. I. and S. U.
Dept. of Eng. Mech.
Blacksburg, VA 24061
Attn: R. H. Heller
H. J. Brinson
C. T. Herakovich
K. L. Reifsnider